Available online at www.sciencedirect.com
SCIENCE DIRECT
International Journal of Heat and Fluid Flow 27 (2006) 627–635
International Journal of HEAT AND FLUID FLOW
www.elsevier.com/locate/ijhff

A subgrid Lagrangian stochastic model for turbulent passive and reactive scalar dispersion

Cesar Aguirre [a], Armando B. Brizuela [a], Ivana Vinkovic [b,*], Serge Simoëns [b]

[a] Facultad de Ciencias Agropecuarias, Universidad Nacional de Entre Rios, Ruta Pcial 11, Km 10, Oro Verde, Parana, Entre-Rios, Argentina
[b] LMFA UMR CNRS 5509, UCB Lyon I, INSA, ECL, Ecole Centrale de Lyon, 69131 Ecully Cedex, France

Available online 23 March 2006

Abstract

A large-eddy simulation (LES) with the dynamic Smagorinsky–Germano subgrid-scale (SGS) model is used to study passive and reactive scalar dispersion in a turbulent boundary layer. Instead of resolving the scalar transport equation, fluid particles containing scalar are tracked in a Lagrangian way. The Lagrangian velocity of each fluid particle is considered to have a large-scale part (directly computed by the LES) and a small-scale part. The movement of fluid elements containing scalar at a subgrid level is given by a three-dimensional Langevin model. The stochastic model is written in terms of SGS statistics at a mesh level. Diffusion is taken into account by a particle pairing exchange model. A second order, irreversible chemical reaction is considered to take place within each fluid particle. The mixing fraction, that behaves as a passive scalar is compared to the experimental results of [Fackrell, J.E., Robins, A.G., 1982. Concentration fluctuations and fluxes in plumes from point sources in a turbulent boundary layer. J. Fluid Mech. 117, 1–26] and to the LES of [Sykes, R.I., Henn, D.S., 1992. Large-eddy simulation of the concentration fluctuations in a dispersing plume. Atmos. Environ. 26A, 3127–3144]. A model for the intensity of segregation is presented and the results of the computations are in good agreement with the model. Finally, the spatial evolution of the intensity of segregation is compared to the dynamic and reactive scalar LES of [Meeder, J.P., Nieuwstadt, F.T.M., 2000. Large-eddy simulation of the turbulent dispersion of a reactive plume from a point source into a neutral atmospheric boundary layer. Atmos. Environ. 34, 3563–3573].

Keywords: Reactive scalar dispersion; Large-eddy simulation; Subgrid stochastic model; Neutral boundary layer

1. Introduction

Owing to an increasing interest in environmental problems, considerable attention has been focused on the prediction of concentration levels downwind of polluting sources in turbulent boundary layers. Since the pioneering work of Deardorff (1970), LES has become a well established tool for the study of turbulent flows (Meneveau and Katz, 2000), the transport of passive scalars (Sykes and Henn, 1992; Kemp and Thomson, 1996) as well as the dispersion of reactive plumes (Sykes et al., 1992; Meeder and Nieuwstadt, 2000). Current LES of scalar fields are increasingly applied to the study of atmospheric dispersion of pollutants, to the evaluation of mixing and segregation rates (Meeder and Nieuwstadt, 2000) or concentration peaks (Xie et al., 2004). However, these Eulerian approaches are less employed when it comes to computing the concentration variance or the SGS characteristics of the scalar field. In this study, a Lagrangian stochastic model is coupled with a LES with the dynamic Smagorinsky–Germano SGS model (Germano et al., 1991), in order to obtain concentration field fluctuations, scalar fluxes and the intensity of segregation of the reactive species.

In order to model the velocity field that advects the fluid elements at a subgrid level, the three-dimensional Langevin equation model (Thomson, 1987), is written in terms of the local SGS characteristics. By this way, the Lagrangian stochastic model is entirely given by the quantities directly computed by the LES with the dynamic Smagorinsky–Germano

* Corresponding author. Tel.: +33 4 72 18 62 05; fax: +33 4 78 64 71 45.
E-mail address: ivana.vinkovic@ec-lyon.fr (I. Vinkovic).

0142-727X/$ - see front matter © 2006 Elsevier Inc. All rights reserved.
doi:10.1016/j.ijheatfluidflow.2006.02.011

SGS model, Germano et al. (1991). Scalar diffusion is taken into account by a particle pairing exchange model, Simoëns et al. (1997) and a second order, irreversible chemical reaction is considered to take place within each fluid particle.

The results of the computations are compared with the wind-tunnel dispersion results of Fackrell and Robins (1982) and with the LES of Sykes and Henn (1992), who used a Lagrangian puff scheme for the scalar transport equation together with a non dynamic SGS model. The intensity of segregation is then computed and a model for this quantity is presented (Simoëns, 2002). Finally, the spatial evolution of the intensity of segregation is compared to the dynamic and reactive scalar LES of Meeder and Nieuwstadt (2000).

2. Large-eddy simulation

A turbulent boundary layer flow is computed using the LES code ARPS 4.5.2. (Xue et al., 2000, 2001). Details of the resolved equations and subgrid closure are given in Aguirre (2005) and in Vinkovic et al. (in press). The continuity and momentum equations obtained by grid filtering the Navier–Stokes equations are:

$$\frac{\partial \tilde{u}_i}{\partial x_i} = 0,$$
$$\frac{\partial \tilde{u}_i}{\partial t} + \tilde{u}_j \frac{\partial \tilde{u}_i}{\partial x_j} = -\frac{1}{\rho}\frac{\partial \tilde{p}}{\partial x_i} + \frac{\partial}{\partial x_j}\left(\nu\left(\frac{\partial \tilde{u}_i}{\partial x_j} + \frac{\partial \tilde{u}_j}{\partial x_i}\right) - \tau^r_{ij}\right) + \tilde{B}_i, \tag{1}$$

where u_i is the fluid velocity, p is the total pressure, ν the molecular kinematic viscosity, ρ the density and $i = 1,2,3$ refers to the x (streamwise), y (spanwise), and z (normal) directions respectively. B_i includes the gravity and the Coriolis force. The tilde denotes application of the grid filtering operation. The dynamic Smagorinsky–Germano subgrid-scale model (Germano et al., 1991) is used.

The dimensions of the computational domain in the streamwise, spanwise and wall-normal directions are, respectively, $l_x = 6H$, $l_y = 3H$ and $l_z = 2H$, H being the boundary layer depth. The Reynolds number based on the friction velocity and the boundary layer depth is $Re = 15{,}040$. The grid is uniform in the xy-planes and stretched in the z-direction by a hyperbolic tangent function. The grid spacings are $\Delta_x = 0.083H$, $\Delta_y = 0.083H$ and $0.0025H < \Delta_z < 0.083H$.

The motion of fluid particles is obtained from

$$\frac{\mathrm{d}x_i}{\mathrm{d}t} = v_i \tag{2}$$

x_i is the position and v_i is the Lagrangian velocity of the fluid particle, given by

$$v_i(t) = \tilde{u}_i(\vec{x}(t)) + v'_i(t) \tag{3}$$

This velocity is considered to have an Eulerian large-scale part $\tilde{u}_i(\vec{x}(t))$ (which is known) and a fluctuating SGS contribution $v'_i(t)$, which is obtained by the stochastic model described in the following section. The Lagrangian large-scale velocities are obtained by a tri-linear quadratic Lagrange interpolation method with 27 nodes. A second-order Runge–Kutta method is used for the time-integration of Eq. (2). At the boundaries, in the x-direction, particles that leave the domain are re-introduced at the source. In the y-direction the periodic boundary conditions are used. Particles that reach the ground rebound respecting symmetric conditions.

3. Subgrid Lagrangian stochastic model

A full description of the coupling between the LES and the subgrid stochastic model may be found in Vinkovic et al. (2005). Only the main features will be presented in this section. The movement of fluid elements containing scalar at a subgrid level is given by a three-dimensional Langevin model:

$$\begin{cases} \mathrm{d}v_i = (\gamma_i(\vec{x},\vec{v},t) + \alpha_{ij}(\vec{x},t)(v_j - \tilde{u}_j))\,\mathrm{d}t + \beta_{ij}(\vec{x},t)\,\mathrm{d}\eta_j(t) \\ \mathrm{d}x_i = v_i\,\mathrm{d}t \end{cases} \tag{4}$$

where $\mathrm{d}\eta_j$ is the increment of a vector-valued Wiener process with zero mean, $\langle \mathrm{d}\eta_j \rangle = 0$, and variance $\mathrm{d}t$, $\langle \mathrm{d}\eta_i \mathrm{d}\eta_j \rangle = \mathrm{d}t\delta_{ij}$. The fluid particle velocity is given by a deterministic part $\gamma_i + \alpha_{ij}v'_j$ and by a completely random part $\beta_{ij}\mathrm{d}\eta_j$. Within the deterministic term, γ_i stands for the large-scale velocity contribution, while $\alpha_{ij}v'_j$ stands for the fluctuating SGS velocity of the fluid particle.

The coefficients α_{ij}, β_{ij} and γ_i are determined by relating the subgrid statistical moments of $\vec{v}'(t)$ to the filtered Eulerian moments of the fluid velocity $\vec{u}(\vec{x},t)$, in analogy with van Dop et al. (1986) who developed this approach in the case of a classic Reynolds averaged decomposition. Assuming that the subgrid turbulence is homogeneous and isotropic, the fluid velocity given by the modified Langevin model writes as

$$\mathrm{d}v_i = \left[\frac{\partial \tilde{u}_i}{\partial t} + \frac{\partial(\tilde{u}_i\tilde{u}_j)}{\partial x_j} + \frac{\partial \tau^r_{ij}}{\partial x_j} + \frac{3}{2}\frac{v_i - \tilde{u}_i}{\tilde{k}}\left(\frac{1}{3}\frac{\mathrm{d}\tilde{k}}{\mathrm{d}t} - \frac{C_0\tilde{\varepsilon}}{2}\right)\right]\mathrm{d}t + \sqrt{C_0\tilde{\varepsilon}}\,\mathrm{d}\eta \tag{5}$$

where $\tilde{k}$ is the subgrid turbulent kinetic energy, $\tilde{\varepsilon}$ is the subgrid turbulent dissipation rate and C_0 is the Lagrangian constant.

The large-scale velocity of the fluid particle is directly computed by the LES with the dynamic Smagorinsky–Germano SGS model. In order to determine the SGS contribution (α_{ij} and β_{ik}) we need to resolve an additional transport equation for $\tilde{k}$. This equation is deduced from Deardorff (1980)

$$\frac{\partial \tilde{k}}{\partial t} + \tilde{u}_j\frac{\partial \tilde{k}}{\partial x_j} = \frac{K_m}{3}\frac{g}{\theta_0}\frac{\partial \tilde{\theta}}{\partial z} + 2K_m\tilde{S}^2_{ij} + 2\frac{\partial}{\partial x_j}\left(K_m\frac{\partial \tilde{k}}{\partial x_j}\right) + \tilde{\varepsilon} \tag{6}$$

where $\tilde{\varepsilon} = C_\varepsilon\tilde{k}^{3/2}/\tilde{\Delta}$. The terms on the right-hand side of Eq. (6) correspond to the production by buoyancy, the pro-

duction by shear, the diffusion of $\tilde{k}$ and the dissipation. Since we are interested in neutral flows the potential temperature variation is neglected. The turbulent eddy viscosity K_m is computed by a dynamic procedure as described in the previous section.

4. The diffusion model

In order to take diffusion into account a deterministic, continuous in time pairing particle exchange model is used. A full description of this model can be found in Simoëns et al. (1997). We will resume here only the main aspects.

The domain is divided in boxes that are small compared to the length scale of the flow (Pope, 1985). In each box, at each time step, particles are randomly selected by pairs. For each pair (m,n), the particle concentrations $C^m(t)$ and $C^n(t)$ will evolve according to

$$\begin{cases} \frac{dC^m(t)}{dt} = \psi(C^n(t) - C^m(t)) \\ \frac{dC^n(t)}{dt} = \psi(C^m(t) - C^n(t)) \end{cases} \tag{7}$$

ψ is a relaxation coefficient. From a theoretical analysis ψ is chosen so that the PDF p_c of the concentration tends to a Gaussian function in isotropic turbulence. As suggested by Spalding (1971), ψ can be expressed as $\psi = \xi/T_{\text{diff}}$, where ξ is a random number between -1 and 1, and the diffusion time T_{diff} can be written as $T_{\text{diff}} = T/C_{\text{diff}}$, with C_{diff} a constant and T the time scale of the velocity fluctuations defined as $T = k/\varepsilon$. Pope (1985) explained that C_{diff} has to be adjusted with the relaxation of the standard deviation of the concentration level σ_c. Even though Pope (1985) suggested a value of 2, Michelot (1996) proposed a value of 2.25 as more appropriate.

5. The chemical reaction

The chemical reaction considered is a second order, irreversible reaction without influence on the turbulent field. Let A and B be two reactive species that undergo the following reaction $A + B \rightarrow C$ at a rate k_r. k_r is assumed constant.

The chemical reaction will take place within each fluid particle. Thus, each particle in a mixing box will carry three scalars A, B and C. If we consider the mth tracked fluid particle, the respective concentrations of the three scalars carried by the particle will be C_A^m, C_B^m and C_C^m. The time evolutions of the concentrations due to chemical reaction are given by the following system:

$$\begin{cases} \frac{dC_A^m(t)}{dt} = -k_r C_A^m C_B^m \\ \frac{dC_B^m(t)}{dt} = -k_r C_A^m C_B^m \\ \frac{dC_C^m(t)}{dt} = +k_r C_A^m C_B^m \end{cases} \tag{8}$$

The generalization to a nth order reversible or non reversible reaction is straightforward. This way, the entire simulation associates turbulent dispersion (LES and subgrid stochastic model), mixing and diffusion (Eq. (7)) and a chemical reaction (Eq. (8)).

6. Model predictions and discussion

6.1. Description of the simulated experiment

A full description of the experimental facility and results can be found in Fackrell and Robins (1982). Here, the main characteristics of the experiment necessary for understanding the simulations are given.

A turbulent boundary layer over a rough wall is generated in an open-circuit wind tunnel. A plume from a point source at $z_s/H = 0.19$ is studied. The source has a 8.5 mm diameter and it emits at the average velocity of the flow over its height. The source gas consists only of a neutrally buoyant mixture of propane and helium. The former is used as a trace gas for concentration measurements. Fackrell and Robins (1982) measured the mean concentration, the concentration fluctuations and the fluxes in the passive scalar plume.

In our simulations, a chemical reaction is introduced. It is a second order irreversible reaction as described in the previous section. In the absence of ultra violet radiation, nitrogen monoxide and ozone undergo the following reaction:

$$\text{NO} + \text{O}_3 \rightarrow \text{NO}_2 + \text{O}_2 + 200\,\text{kJ/mole} \tag{9}$$

The reaction rate k_r is constant at 293 K, $k_r = 0.37\ \text{ppm}^{-1}\,\text{s}^{-1}$. In order to compare the results of the simulation with the reference experiment, the mixing fraction F is computed. The mixing fraction is defined by

$$F = \frac{C_{\text{NO}} - C_{\text{O}_3} + C^0_{\text{O}_3}}{C^0_{\text{NO}} + C^0_{\text{O}_3}} \tag{10}$$

C_{NO} and C_{O_3} represent the concentrations of nitrogen monoxide and ozone respectively. The superscript (0) indicates initial values. The mixing fraction F behaves as a passive scalar if the diffusivities of the individual scalars are the same. By computing the behavior of F we can obtain the characteristics of the passive scalar plume as measured by Fackrell and Robins (1982).

In the computation particles containing nitrogen monoxide are continuously ejected from the source. Ten particles are ejected at each time step until the number of particles in the domain becomes constant. Around the plume of nitrogen monoxide there are ozone particles. Therefore, at the same instant fluid particles containing ozone are introduced in the domain. Since for the chemical reaction it has to be always enough ozone, for each particle of nitrogen monoxide, 10 particles of ozone are added. Ozone particles are rejected around the plume source and in every mixing box where ozone particles lack, new are injected.

The LES (Eq. (1)) coupled with the subgrid stochastic model (Eq. (5)) and the diffusion model (Eq. (7)) has

already been applied to the study of passive scalar dispersion, Vinkovic et al. (in press). Details of the boundary layer flow such as mean velocity, turbulent kinetic energy and fluctuation profiles can be found in Vinkovic et al. (in press). Here we will only describe the results relative to reactive scalar dispersion.

6.2. Mixing fraction profiles

The vertical profiles of the mean mixing fraction $\overline{F}$ at $x = 0.96H$, $x = 1.92H$ and $x = 2.88H$ from the source are shown on Fig. 1. The computed mean mixing fraction profiles are in good agreement with the experimental results of Fackrell and Robins (1982) and with the vertical profiles of the mean concentration obtained in the passive scalar case. The results are also compared with the LES of Sykes and Henn (1992). Sykes and Henn simulated the experiment of Fackrell and Robins (1982) with a Lagrangian puff scheme for the scalar transport equation. As we move away from the source, the simulations of Sykes and Henn (1992) underestimate the mean concentration near the wall.

The vertical profiles of the standard deviation of the mixing fraction, $\overline{F'^2}$, normalized by its maximum value are illustrated in Fig. 2, showing close agreement with the experimental data. The difference between the passive and the reactive scalar case is more important here and the profiles of $\overline{F'^2}$ are closer to the experimental results. Since fluid particles containing ozone are injected continuously into the computational domain (as explained above), in the case of the reactive scalar computations, there are two times more particles than in the passive scalar case. This is the reason why the standard deviation profiles for the mixing fraction are in better agreement with the experimental results.

Fig. 3 shows the vertical velocity mixing fraction correlation profiles, $\overline{w'F'}$, at $x = 0.96H$, $x = 1.92H$ and $x = 2.88H$. In the figure $C_{\max}$ and $F_{\max}$ are the local maximum concentration and mixing fraction for each profile, respectively. The evolution of the profile shapes is in good agreement with the experimental data. The flux profiles develop from being antisymmetric about the source height near the source, toward a ground-level source profile. Differences appear between the passive and the reactive scalar case. For the passive scalar, our simulations tend to overestimate the mass flux, particularly far from the wall. The profiles obtained in the reactive scalar case tend to underestimate the vertical velocity mixing fraction correlation both near the wall and far from the wall as we move away from the source.

6.3. Mean concentration profiles of reactive species

The vertical profiles of the mean concentration of the reactive species NO, O_3 and $NO_2 + O_2$ at different distances from the source are shown in Fig. 4. The profiles are normalized by the local maximum concentration for each specie and each profile. The figures show clearly the existence of two regimes. Near the source (up to $x \sim 2H$), the peak of maximum concentration of the product of the reaction ($NO_2 + O_2$) is at the same vertical position as the peak of maximum concentration of the reacting specie injected at the source (NO).

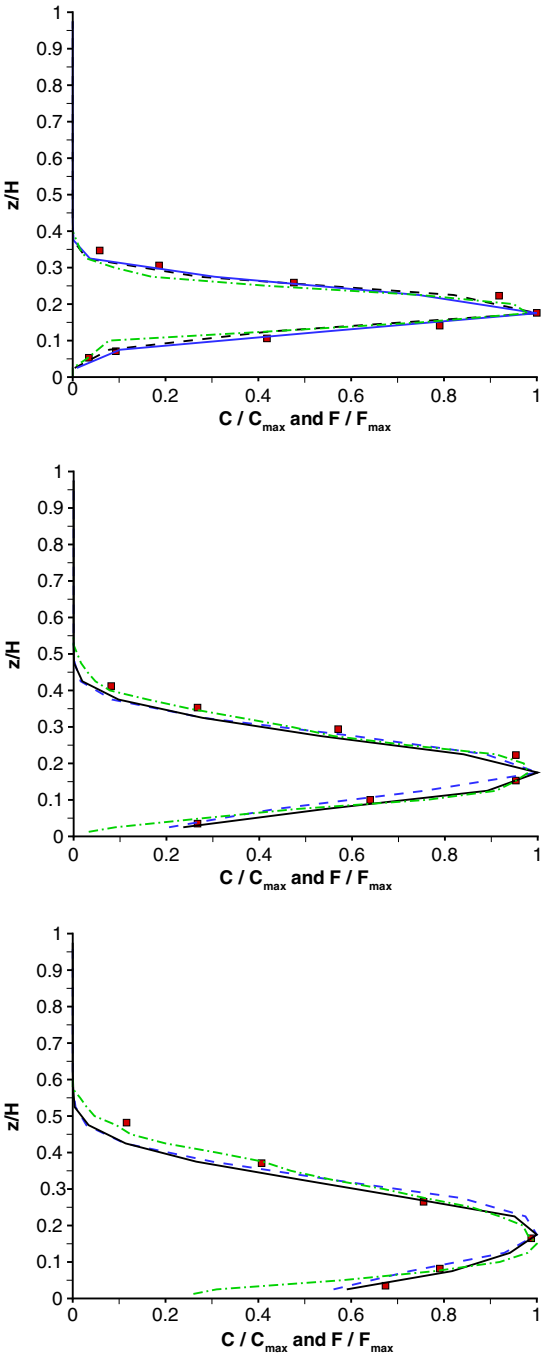

Fig. 1. Mean concentration $\overline{C}$ and mixing fraction $\overline{F}$ at $x = 0.96H$, $x = 1.92H$ and $x = 2.88H$. Full line – $\overline{F}$ our simulations; dashed – $\overline{C}$ our simulations; dashed-dotted – $\overline{C}$ LES of Sykes and Henn (1992); squares – $\overline{C}$ Fackrell and Robins (1982).

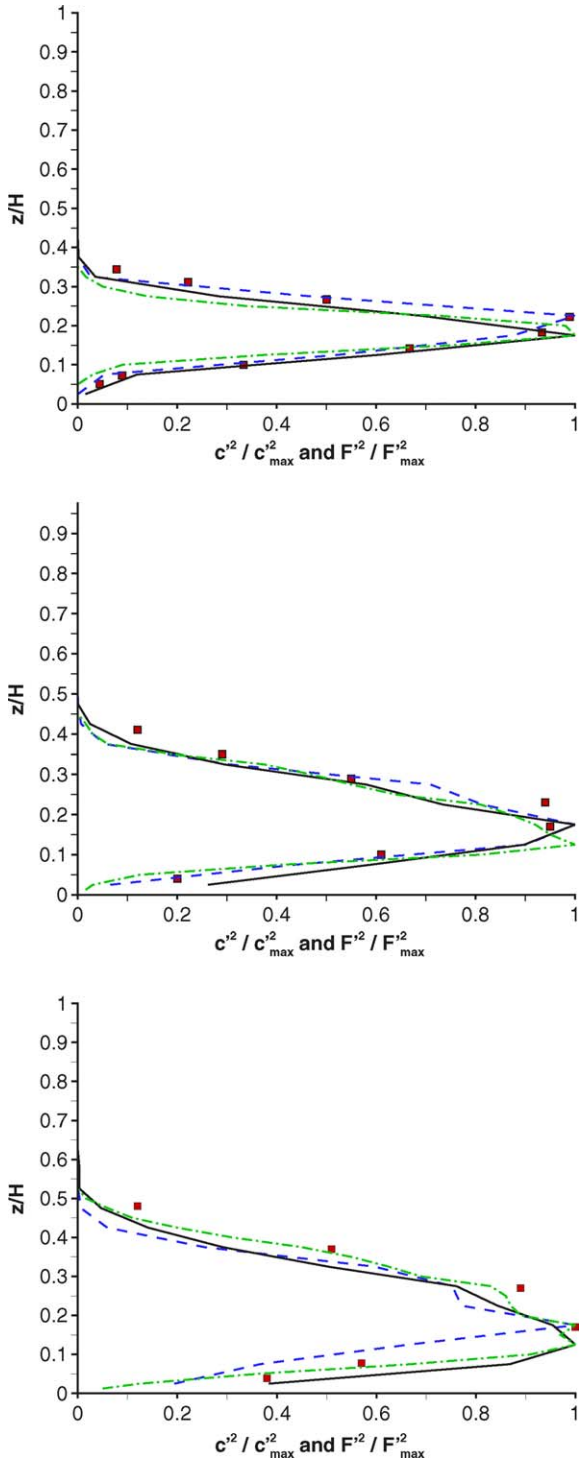

Fig. 2. Mean-square concentration $\overline{C'^2}$ and mean-square mixing fraction $\overline{F'^2}$ at $x = 0.96H$, $x = 1.92H$ and $x = 2.88H$. Full line – $\overline{F'^2}$ our simulations; dashed – $\overline{C'^2}$ our simulations; dashed-dotted – $\overline{C'^2}$ LES of Sykes and Henn (1992); squares – $\overline{C'^2}$ Fackrell and Robins (1982).

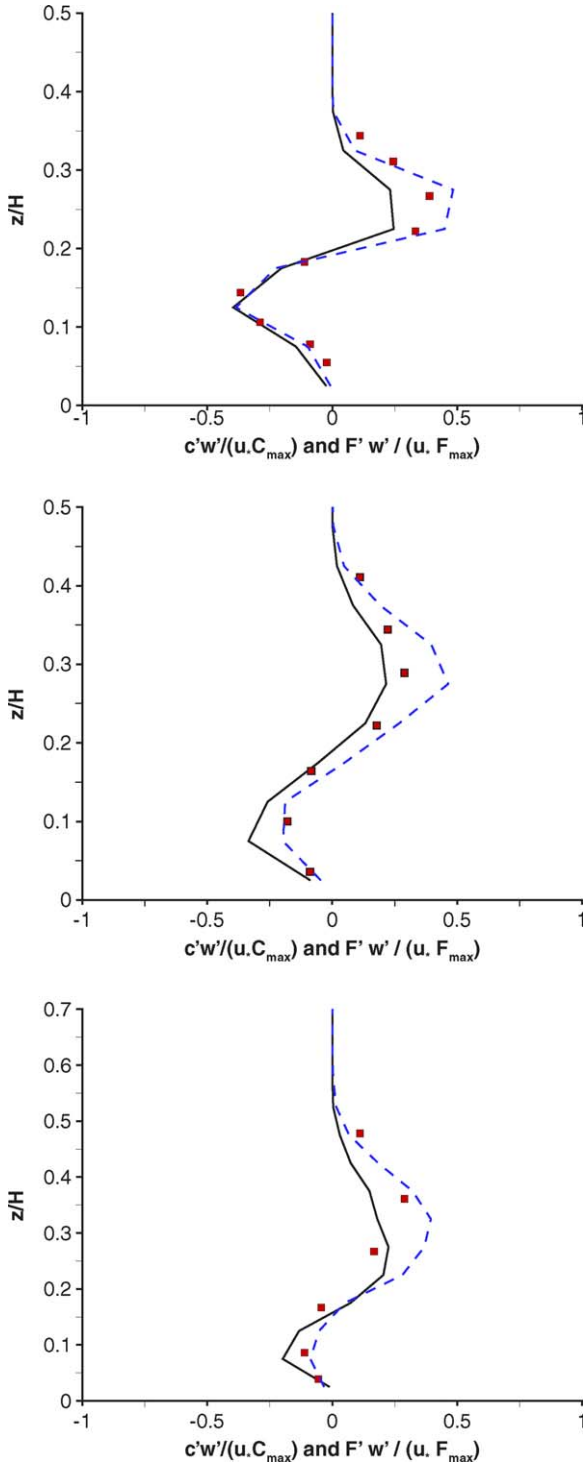

Fig. 3. Mass flux $\overline{w'C'}$ and velocity mixing fraction correlation $\overline{w'F'}$, at $x = 0.96H$, $x = 1.92H$ and $x = 2.88H$. Full line – $\overline{w'F'}$ our simulations; dashed – $\overline{w'C'}$ our simulations; squares – $\overline{w'C'}$ Fackrell and Robins (1982).

Away from the source ($x \geqslant 2.88H$), a first peak of maximum concentration of $NO_2 + O_2$ appears at the upper boundary of the NO plume, and a second peak is present slightly above the maximum concentration peak of NO.

6.4. Intensity of segregation

Fig. 5 illustrates the vertical profiles of the intensity of segregation I_s, given by

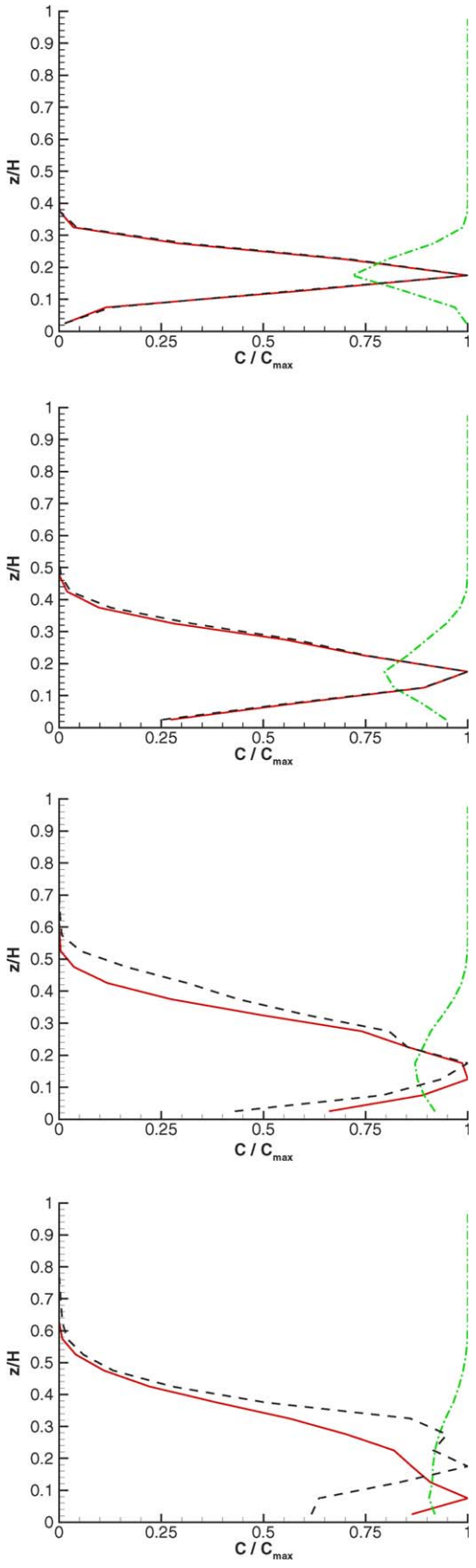

Fig. 4. Mean concentration of NO, O_3 and $NO_2 + O_2$ at $x = 0.96H$, $x = 1.92H$, $x = 2.88H$ and $x = 3.83H$. Full line – NO; dashed-dotted – O_3; dashed – $NO_2 + O_2$.

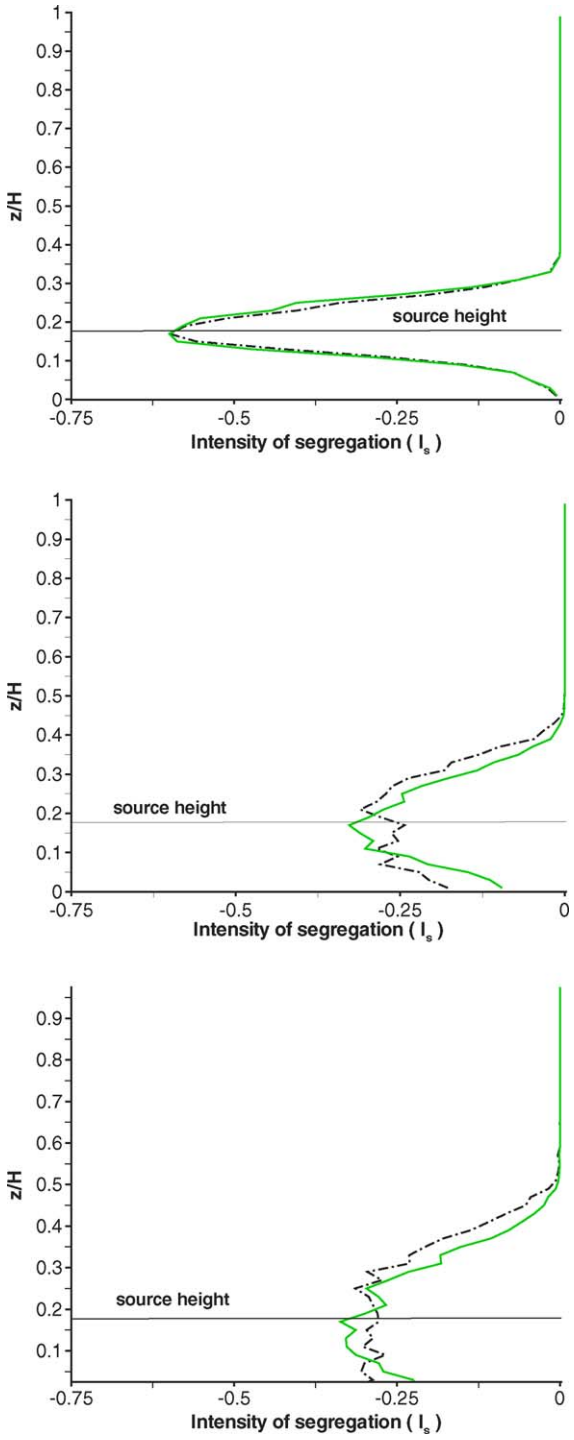

Fig. 5. Intensity of segregation I_s at $x = 0.96H$, $x = 1.92H$ and $x = 2.88H$. Full line – our simulations; dashed-dotted – gradient model (Eq. (17)).

$$I_s = \frac{\overline{C'_{NO} C'_{O_3}}}{\overline{C}_{NO} \overline{C}_{O_3}} \tag{11}$$

at three different distances from the source. As expected, since NO and O_3 are not pre-mixed near the source, the intensity of segregation is negative.

Because few experiments with reactive scalar giving the intensity of segregation exist, it is interesting to have

another element of comparison than the LES of Meeder and Nieuwstadt (2000). This is the reason why we used the following model for the intensity of segregation. The explanation and comparisons may be found in Simoëns (2002). Let m be a fluid particle containing a specie A which has an instantaneous concentration $C^m(z_0 + dz)$ at location $z_0 + dz$. We suppose that there is a mean gradient of concentration at this location. Such an assumption is not absurd when the mixing is not total. Following the hypothesis and the Reynolds decomposition the particle m has a fluctuation $C'^m(z_0 + dz)$ equal to the difference between mean concentration at $z_0 + dz$, $\overline{C}(z_0 + dz)$, and the mean concentration $\overline{C}(z_0)$:

$$C'^m(z_0 + dz) = \overline{C}(z_0 + dz) > -\overline{C}(z_0) \tag{12}$$

If $dz \ll 1$, we will have

$$\overline{C}(z_0) \sim \overline{C}(z_0 + dz) - dz\frac{\partial \overline{C}(z_0)}{\partial z} \tag{13}$$

Thus

$$C'^m(z_0 + dz) \sim dz\frac{\partial \overline{C}(z_0)}{\partial z} \tag{14}$$

By applying the same procedure for two species we obtain

$$C'^m_A(z_0 + dz)C'^m_B(z_0 + dz) \sim dz^2\frac{\partial \overline{C}_A(z_0)}{\partial z}\frac{\partial \overline{C}_B(z_0)}{\partial z} \tag{15}$$

Therefore, we can deduce that

$$\overline{C'^m_A C'^m_B}(z_0 + dz) \sim dz^2\frac{\partial \overline{C}_A(z_0)}{\partial z}\frac{\partial \overline{C}_B(z_0)}{\partial z} \tag{16}$$

and thus

$$I_s \sim \frac{D_s}{\overline{C}_A\overline{C}_B}\frac{\partial \overline{C}_A}{\partial z}\frac{\partial \overline{C}_B}{\partial z} \tag{17}$$

where D_s is a diffusion coefficient that depends on z.

Directly computed values of I_s are compared with the values calculated from Eq. (17) in Fig. 5. The diffusion coefficient D_s was chosen to obtain the best fit. A double peak on the vertical profile through the plume centerline of I_s appears. The double peak exists both for the gradient model as for Lagrangian stochastic modeling, even though for this last case it is less evident. This double peak is also present in the Eulerian subgrid-scale modeling by Meeder and Nieuwstadt (2000). It is not clear why such peak appear. Probably it is due to the inflexion points of the vertical profile of $\overline{C}_{O_3}$, which are not located at the same height as the inflexion points of $\overline{C}_{NO}$. This difference in the position of the inflexion points also appears for the results of Meeder and Nieuwstadt (2000). As we move downstream of the source, for the results of Meeder and Nieuwstadt (2000) as for our simulations, the profiles of NO and O_3 become more similar even when they are perturbated by the presence of the wall. Probably the influence of the wall (producing asymmetry) is stronger on the spreading of O_3 than on the species ejected from the source.

The evolution of the D_s with distance from the source is illustrated on Fig. 6. It is interesting because it shows two

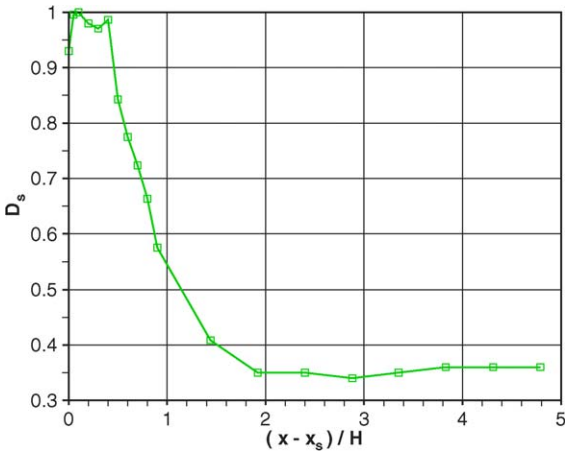

Fig. 6. Diffusion coefficient D_s as function of x.

different regimes of reactive scalar mixing. Close to the source ($x \leqslant 1.92H$), D_s decreases significantly. At $x \sim 2H$, D_s attains a constant value, representing the change of mixing regime. There are two phases (or regions) before D_s attains a constant value. The first one, near the source is for high concentration gradient levels for both original species. The turbulence effect are not too high and the advection determines the spreading and thus the segregation. The second region could be defined as an equilibrium region where the stress tensor and the turbulent kinetic energy balance the mean concentration gradient. Thus, the behavior of D_s in this region has to combine both effects. It would be interesting, in a future work, to compare this proposed modeling of the segregation to a more complex modeling as the one proposed by Meeder and Nieuwstadt (2000).

6.5. Comparison with the simulations of Meeder and Nieuwstadt (2000)

In this section, the intensity of segregation obtained by our simulations and by the model (Eq. (17)) is compared to the value computed by Meeder and Nieuwstadt (2000). Meeder and Nieuwstadt (2000) studied the dispersion of NO from a point source in a neutral atmospheric boundary layer of O_3. They used a LES with a 1.5 turbulent kinetic energy subgrid-scale model and a completely Eulerian approach for the transport equation of the intensity of segregation. The wind tunnel observations of Builtjes (1983) were used as a test case by the authors.

Table 1 shows the characteristics of our simulations (OS), compared to the LES of Meeder and Nieuwstadt (2000) (M&N2000) and the experiments of Builtjes (1983) (B83). The Damköhler number was computed by

$$\begin{cases} Da_{NO} = k_r C^0_{O_3}\left(\frac{z_s}{U_s}\right) \\ Da_{O_3} = k_r C^0_{NO}\left(\frac{A_s}{U_s z_s}\right) \end{cases} \tag{18}$$

Table 1
Characteristics of the experiments of Builtjes (1983) (B83), the LES of Meeder and Nieuwstadt (2000) (M&N2000) and our simulations (OS)

	k_r (ppm^{-1} s^{-1})	C^0_{NO}(ppm)	$C^0_{O_3}$(ppm)	Da_{NO}	Da_{O_3}
B83	0.40	3900.0	0.35	0.049	0.196
M&N2000	0.01	55.0	0.35	0.051	0.192
OS	0.37	515.0	1.00	0.027	0.015

	A_s (mm^2)	U_s (m/s)	z_s (m)	z_0 (m)
B83	7.06	0.40	0.140	9.95×10^{-5}
M&N2000	301.06×10^6	7.70	112.000	9.97×10^{-2}
OS	56.69	3.18	0.228	2.88×10^{-4}

where z_s and A_s are the height and the area of the source, respectively, U_s is the velocity of the flow at the source position and z_0 is the surface roughness. The Damköhler numbers in the experimental case of Builtjes (1983) and in the LES of Meeder and Nieuwstadt (2000) are close. In our simulations both Da_{NO} and Da_{O_3} are lower, illustrating the fact that in our case the chemical reaction is slower. Therefore, close to the source we expect to obtain a lower intensity of segregation.

The spatial evolution of the intensity of segregation I_s obtained by our simulations and compared to the LES of Meeder and Nieuwstadt (2000) is shown in Fig. 7. Near the source, in our simulations, the chemical reaction is moderated ($I_s \sim -1$). As the distance increases, I_s tends towards 0 and at $x \sim H$ it attains a constant value of $I_s \sim -0.3$, illustrating the fact, that in our case the chemical reaction is slow. In the case simulated by Meeder and Nieuwstadt (2000) the chemical reaction is slow near the source. The intensity of segregation is close to 0 near the source and then decreases up to $I_s \sim -0.45$ at $x \sim H$, attaining $I_s \sim -0.3$ progressively, further downstream.

The model presented above (Eq. (17)) is in good agreement with the computed results up to $x \sim H$. As we move away from the source, the differences remain small.

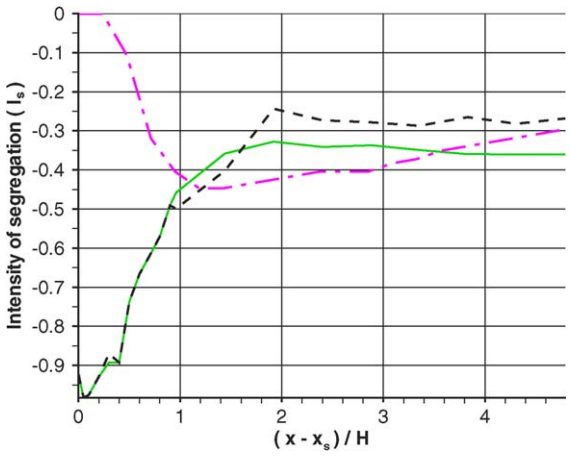

Fig. 7. Intensity of segregation I_s of NO and O_3. Full line – gradient model (Eq. (17)); dashed – our simulations; dashed-dotted – LES of Meeder and Nieuwstadt (2000).

7. Conclusion

A LES coupled with a Lagrangian stochastic model has been applied to the study of reactive scalar dispersion downwind of a localized source of NO. Fluid particles containing scalar are tracked in a Lagrangian way. The Lagrangian velocity of each fluid particle is considered to have a large-scale part and a small-scale part at a subgrid level. The subgrid movement of fluid elements containing scalar is given by a three-dimensional Langevin model using the filtered SGS statistics in inhomogeneous turbulence. Diffusion is taken into account by a deterministic, continuous in time pairing particle exchange model. A second order, irreversible chemical reaction is considered to take place within each fluid particle.

The mixing fraction, that behaves as a passive scalar is compared to the experimental results of Fackrell and Robins (1982) and to the LES of Sykes and Henn (1992) who used a Lagrangian puff scheme for the scalar transport equation together with a non dynamic SGS model. Good agreement with the experiments is achieved. The mean concentration profiles of the reactive species are computed showing the existence of two different mixing regimes as we move away from the source.

The intensity of segregation is obtained directly from the computed results with no additional simulations or closures. A model for the intensity of segregation is presented and the results of the computations are in good agreement with the model. Finally, the spatial evolution of the intensity of segregation is compared to the LES of Meeder and Nieuwstadt (2000) who used a completely Eulerian approach.

The LES coupled with the Lagrangian stochastic model provides good description of the plumes from elevated sources. Standard deviations of the concentration as well as higher order moments or the intensity of segregation are directly obtained from the computed results with no additional closures. Multiple chemical reactions can be easily included without additional scalar equations. Phenomena taking place at the source can be described with no new grid refinement.

References

Aguirre, C., 2005. Dispersion et mélange atmosphérique euléro—Lagrangien de particules fluides réactives. Application à des cas simples et complexes. Thèse de doctorat de L'Université Claude Bernard—Lyon I.

Builtjes, P., 1983. In: Wispelaere, C. (Ed.), A Comparison Between Chemically Reacting Plume Models and Wind-tunnel Experiments. Air Pollution Modeling and its Application, vol. II. Plenum Press, New York, pp. 59–84.

Deardorff, J.W., 1970. A numerical study of three-dimensional turbulent channel flow at large Reynolds numbers. J. Fluid Mech. 41, 453–480.

Deardorff, J.W., 1980. Stratocumulus-capped mixed layer derived from a three-dimensional model. Boundary-Layer Meteorol. 18, 495–527.

Fackrell, J.E., Robins, A.G., 1982. Concentration fluctuations and fluxes in plumes from point sources in a turbulent boundary layer. J. Fluid Mech. 117, 1–26.

Germano, M., Piomelli, U., Moin, P., Cabot, W.H., 1991. A dynamic subgrid-scale viscosity model. Phys. Fluids 3, 1760–1765.

Kemp, J.R., Thomson, D.J., 1996. Dispersion in stable boundary layers using large-eddy simulation. Atmos. Environ. 30, 2911–2923.

Meeder, J.P., Nieuwstadt, F.T.M., 2000. Large-eddy simulation of the turbulent dispersion of a reactive plume from a point source into a neutral atmospheric boundary layer. Atmos. Environ. 34, 3563–3573.

Meneveau, C., Katz, J., 2000. Scale-invariance and turbulence model for large-eddy simulation. Annu. Rev. Fluid Mech. 32, 1–32.

Michelot, C., 1996. Développement d'un modèle stochas-tique Lagrangien: application à la dispersion et à la chimie de l'atmosphère. Thèse de doctorat de L'Ecole Centrale de Lyon.

Pope, B.S., 1985. PDF methods for turbulent reactive flows. Prog. Energy Combust. Sci. 11, 119–192.

Simoëns, S., 2002. De la méthode pour l'étude de la dispersion du mélange de scalaire passif ou réactifHabilitation á diriger des recherches. Université Claude Bernard, Lyon I.

Simoëns, S., Michelot, C., Ayrault, M., Sabelnikov, V., 1997. Modèle stochastique de diffusion continu en temps. CR Mécanique 324, 667–678.

Spalding, D.B., 1971. Concentration fluctuations in a round turbulent free jet. Chem. Eng. Sci. 26, 95–107.

Sykes, R.I., Henn, D.S., 1992. Large-eddy simulation of the concentration fluctuations in a dispersing plume. Atmos. Environ. 26A, 3127–3144.

Sykes, R.I., Henn, D.S., Parker, S.F., 1992. Large-eddy simulation of a turbulent reacting plume. Atmos. Environ. 26A, 2565–2574.

Thomson, D.J., 1987. Criteria for the selection of stochastic models of particle trajectories in turbulent flows. J. Fluid Mech. 180, 529–556.

van Dop, H., Nieuwstadt, F.T.M., Hunt, J.C.R., 1986. Random walk models for particle displacement in in-homogeneous unsteady turbulent flows. Phys. Fluids 28, 1639–1653.

Vinkovic, I., Aguirre, C., Simoëns, S., Gence, J.N., 2005. Coupling of a subgrid Lagrangian stochastic model with large-eddy simulation. C.R. Mecanique 333, 325–330.

Vinkovic, I., Aguirre, C., Simoëns, S., in press. Large-eddy simulation and Lagrangian stochastic modeling of passive scalar dispersion in a turbulent boundary layer. J. Turbulence.

Xie, Z., Hayden, P., Voke, R., Robins, A.G., 2004. Large-eddy simulation of dispersion: comparison between elevated and ground-level sources. J. Turbulence 5, 1–16.

Xue, M., Droegemeier, K.K., Wong, V., 2000. The Advanced Regional Prediction System (ARPS)—a multi-scale nonhydrostatic atmospheric simulation and prediction model. Part I: Model dynamics and verification. Meteorol. Atmos. Phys. 75, 161–193.

Xue, M., Droegemeier, K.K., Wong, V., Shapiro, A., Brewster, K., Carr, F., Weber, D., Liu, Y., Wang, D., 2001. The Advanced Regional Prediction System (ARPS)—a multi-scale nonhydrostatic atmospheric simulation and prediction tool. Part II: Model physics and applications. Meteorol. Atmos. Phys. 76, 143–165.